ESKİŞEHİR TECHNICAL UNIVERSITY JOURNAL OF SCIENCE AND TECHNOLOGY A- APPLIED SCIENCES AND ENGINEERING

19th National Clay Symposium (Clay'2023) Sprecial Issue 2023

2023, Vol.24, pp. 33-50, DOI:10.18038/estubtda.1369922

MINERALOGICAL AND GEOCHEMICAL PROPERTIES OF THE MIOCENE ROCKS OUTCROPPING AROUND TUZLUCA (IĞDIR-TÜRKİYE)

Türker YAKUPOĞLU [1,*], Enver KARASU [2]

[1] Department of Geological Engineering, Faculty of Engineering, Van Yüzüncü Yıl University, Van, Türkiye
[2] Iğdır Provincial Disaster and Emergency Directorate, Iğdır, Türkiye

ABSTRACT

In this study, the Miocene lithostratigraphic units (Turabi, Çincavat and Tuzluca formations) outcropping in the Neogene Kağızman-Tuzluca Basin in the west of Iğdır province were studied. The units are represented by evaporitic, carbonate and clayey rocks. This study aims to determine the mineralogical and geochemical properties of these rocks and to interpret the data to evaluate paleodepositional conditions. For this purpose X-ray diffraction (XRD) whole rock and clay fraction, Optical Microscope (OM) studies, X-ray fluorescence (XRF) element identifications and, Field Emission Scanning Electron Microscopy-Energy Dispersive X-ray Spectrometry (FESEM-EDS) analyses of rock samples taken along the sections measured in the field were carried out. Quartz, feldspar, mica, calcite, gypsum and halite minerals were determined in whole rock compositions of the samples. Smectite, illite, chlorite and paligorskite minerals were found in the clay fractions. OM, FESEM-EDS and XRF studies indicate that the origins of gypsum, halite, calcite and palygorskite minerals are authigenic while chlorite, illite, quartz, feldspar and mica were detrital. The predominance of smectite, as well as the presence of chlorite, illite and palygorskite indicate that the basin developed under alkaline conditions, mostly hot and humid, and occasionally arid and cold climates. The positive correlation of SiO_2 with MgO signifies the input of clay and other clastic materials to the basin. While high positive correlation (R^2=0.80) between Zn and Fe_2O_3 indicates the Zn element is of biological origin; high concentrations of Zn, Cu, Ni and Co suggest the high activity of the microorganisms.

Keywords: Tuzluca, XRD, XRF, FESEM-EDS, Origin

1. INTRODUCTION

This study aims to interpret the mineralogical and geochemical properties of the Miocene units (evaporite, claystone, mudstone, sandstone, marl) cropping out near the Tuzluca district of Iğdır province (Türkiye) (Figure 1) in terms of paleodepositional conditions. It is the first comprehensive study on the determination of the whole rock and clay fraction mineralogy of the sedimentary rocks in the Tuzluca section of the Neogene Kağızman-Tuzluca Basin.

Most of the lacustrine basins in Türkiye were formed during the Paleogene and the Neogene periods [1-5]. The Neogene Kağızman-Tuzluca Basin (KTB) is one of the main Cenozoic basins located on the Eastern Anatolian Plateau (Figure 2). Mineralogical [6, 7, 8], geochemical [9], sedimentological [10-13], structural geological [14], and paleontological [15, 16] studies have been carried out in the basin until today. In previous studies regarding basin fill sediments, two different basin models have been proposed: the pull-apart basin [10, 13, 14] and the intermountain basin [11, 12].

In the eastern part of the Kağızman-Tuzluca Basin (Tuzluca section), the basement rocks consist of the Upper Cretaceous ophiolitic rocks (serpentinites), volcanics and marbles.

*Corresponding Author: turkery@yyu.edu.tr
Received: 02.10.2023 Published: 29.11.2023

Formations which constitute the main subject of this study, were firstly divided into three and named by Eşder [6]. Şen et al. [15] established the stratigraphy used today. These are Turabi (Lower Miocene), Çincavat (Middle Miocene) and Tuzluca (Upper Miocene) Formations (Figure 1). The boundaries of these formations are comformable with each other. Turabi Formation, consisting of evaporite, sandstone, claystone and marl, was deposited in environments ranging from fluvial to lake, but mainly in swamp environments. Flood plain sediments, caliche and temporary fluvial sediments form Çincavat Formation which the red color dominates. Evaporites, mudstones and siltstones are the main lithologies of this unit. Tuzluca Formation, which presents thick sequences near Tuzluca, consists mainly of bedded halite and gypsum, which are the product of a shallow saline lake environment. Claystone and marl are interlayered with evaporites.

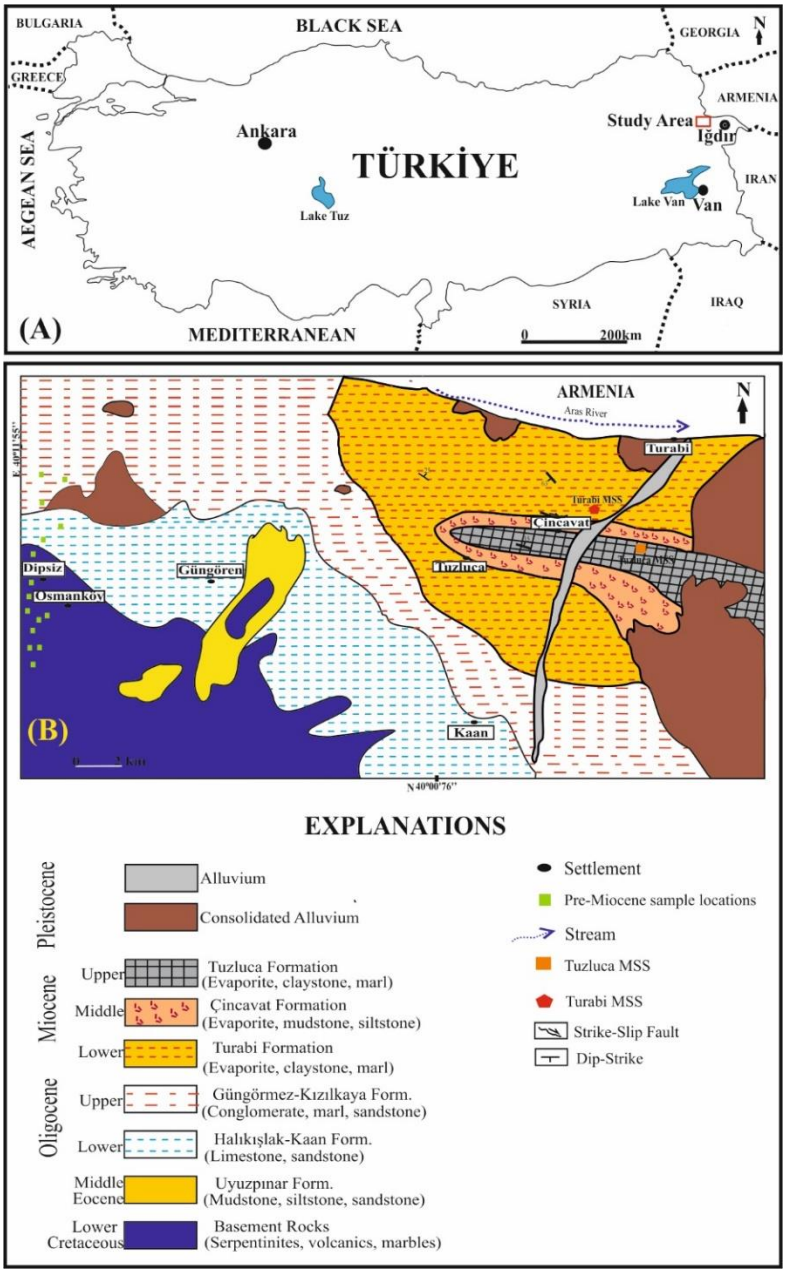

Figure 1. Location map (A) and geological map (B) of the study area (modified from [5])

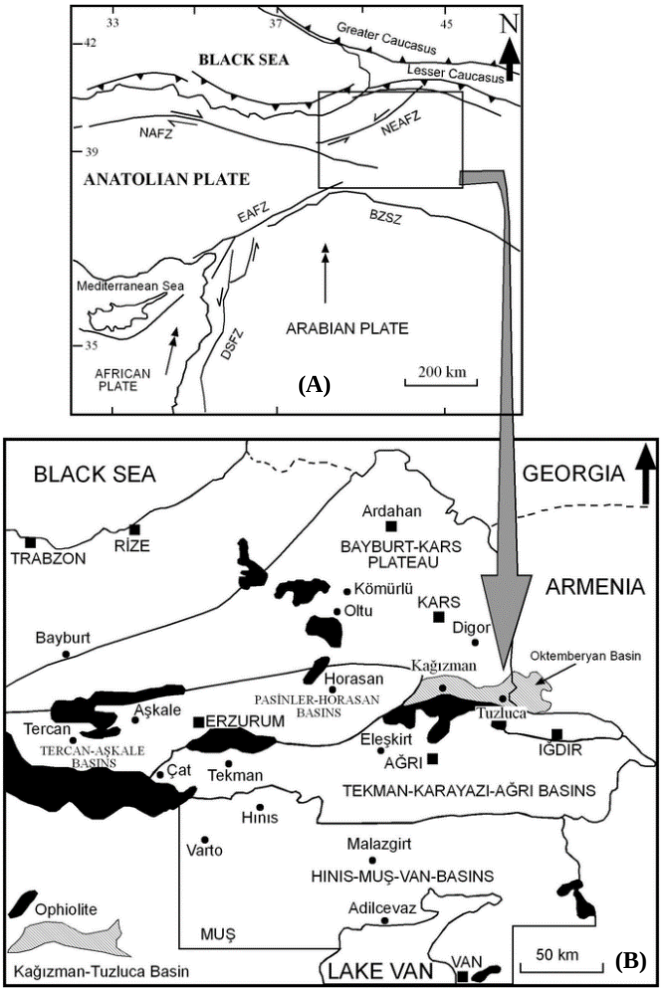

Figure 2. Structural geological elements of Eastern Anatolia (A) (DSFZ Dead Sea Fault Zone, KAFZ North Anatolian Fault Zone, KAFZ Northeast Anatolian Fault Zone, DAFZ Eastern Anatolian Fault Zone, BZSZ Bitlis-Zagros Suture Zone) and location map of Eastern Anatolian basins (B) (Modified from [5])

2. MATERIALS AND METHODS

This study utilized a total of 11 rock samples gathered from the stratigraphic section measured at the Tuzluca salt pit (Figure 3), along with 21 rock samples obtained from the stratigraphic section measured near Turabi village (Figure 4). Additionally, 15 rock samples sourced from pre-Miocene rocks were included in the study material.

Detailed XRD clay analyses of all 32 rock samples taken along measured stratigraphic sections were carried out in the XRD Laboratory of the General Directorate of Mineral Research and Exploration (MTA), Department of Mineral Analysis and Technology. Diffractograms were evaluated with the help of relevant literature and by applying the Hanawalt method [17], and the minerals forming the whole rock and clay fraction of the samples were determined. Semi-quantitative abundances of minerals forming the bulk composition of the rocks were determined using Brindley and Brown [18]. Wilson [19]

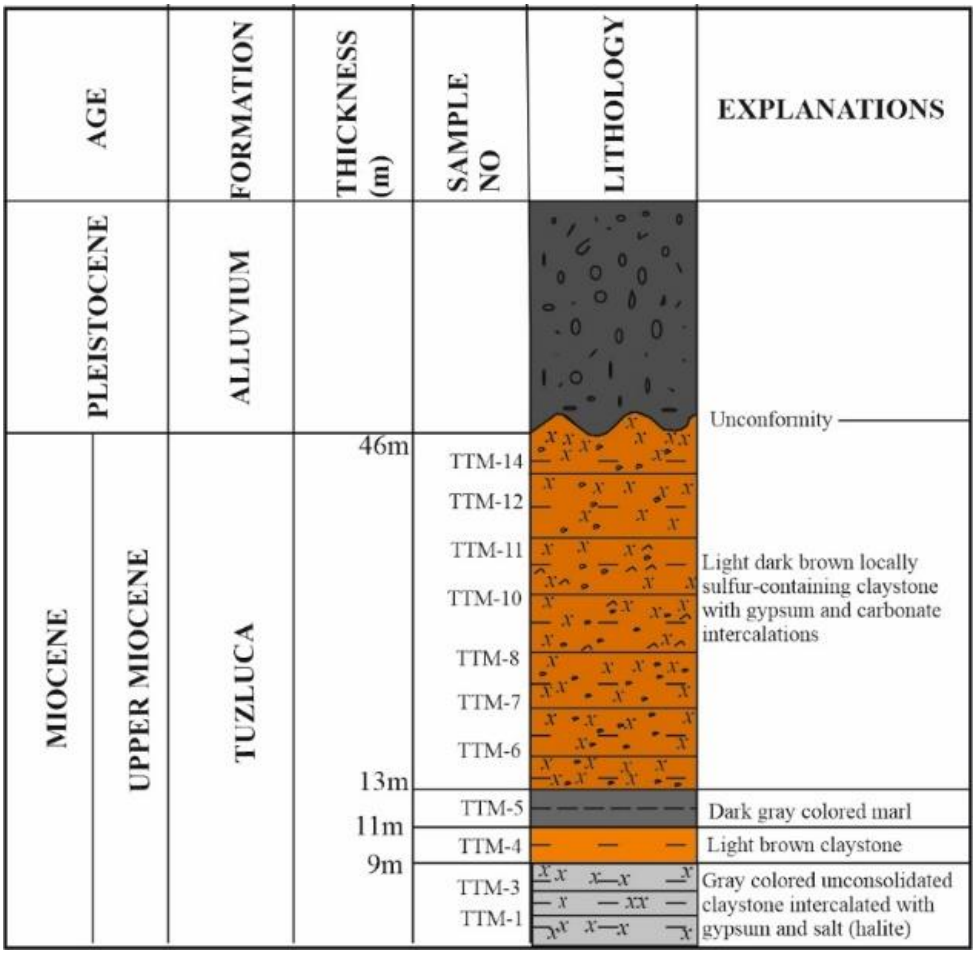

(a)

(b)

Figure 3. Measured stratigraphic section of Tuzluca (salt pit) (a) and a view from the location of section (b)

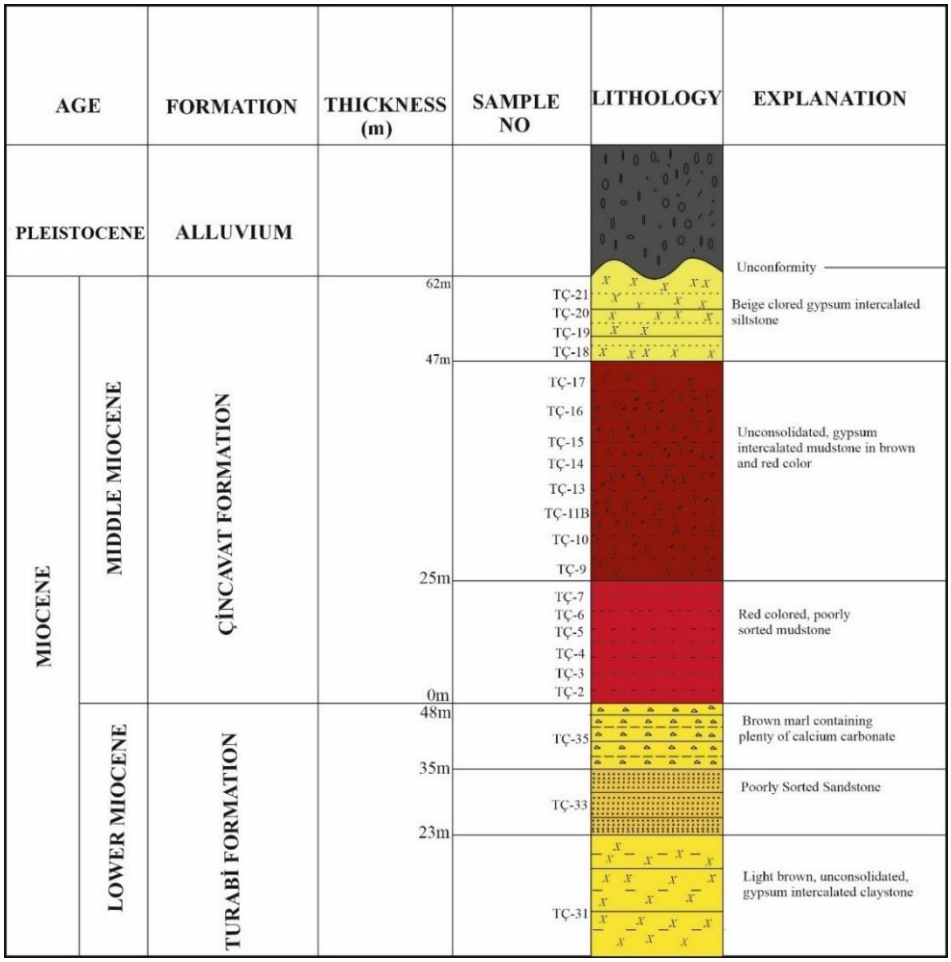

(a)

(b)

Figure 4. Measured stratigraphic section of Turabi village **(a)** and a view from the formations **(b)**

and Moore and Reynolds [20] were used for the abundances, typical reflectances and mineral density factors of clay mineral fractions.

Scanning Electron Microscopy-Energy Dispersive Spectroscopy (SEM-EDS) studies were carried out on 5 selected samples in the SEM laboratory of Van Yüzüncü Yıl University-Science Application and Research Center. In this study, the ZEISS SIGMA 300 model FESEM was used. During FESEM analysis, a Secondary Electron (SE) detector was used, which provides more detailed information about morphological features.

Microchemical analyses were performed with an AMETEK EDAX brand EDX detector connected to the FESEM device. While interpreting SEM and EDS studies, Welton [21] was used as the main reference.

An optical Microscope (OM) study was carried out in order to determine the minerals that make up the rocks and the texture of the rock and the rocks are named. For this purpose, a total of 15 sample thin sections were made at Dokuz Eylül University Torbalı Vocational School Rock Mechanics Laboratory, and they were examined and photographed using a polarizing microscope at Van Yüzüncü Yıl University Geological Engineering Department Microscope Laboratory.

Geochemical analysis of 10 selected samples was carried out at Ankara University Earth Sciences Application and Research Center by X-ray fluorescence (XRF).

3. RESULTS

3.1. Optical Microscope Study

The samples collected from pre-Miocene rocks in the Tuzluca section of the Kağızman-Tuzluca Basin were examined by optical microscope (the sample numbers, rock names, and nicol types are presented in Figure 5). Alterations were observed in almost all of the samples.

In serpentinites, serpentinization developed along pyroxene cracks and fractures, causing the pyroxenes to partially weather. A reticular texture has formed within the rock. Secondary quartz mineral with serpentinization has been formed. Iron oxidation has occurred in rock fractures (Figure 5a). Chloritization (0.1 mm size) is intensely observed in serpentinites (Figure 5b).

In basalts, olivine crystals have a highly fractured and fissured structure. Plagioclases are completely carbonated, and chloritization is observed in pyroxenes (Figure 5c). Plagioclase, pyroxene and olivine phenocrysts are in the matrix consisting of dense volcanic glass (Figure 5d). Calcite mineral is seen as the secondary mineral that fill gas space in the dacite sample (5e). Plagioclase minerals and volcanic glass have completely argilisied, and chloritization has been observed in Mg-Fe silicates (Figure 5e, f).

In the troctolite sample, olivine and plagioclase phenocrysts are evident. A Fe-rich zone was formed in olivine and iddingsitization has taken place. Polysynthetic twinning is observed in plagioclase (Figure 5g).

In the sandstone samples, the cement material is sparite (5h) or micrite (5j) and iron oxidation alteration has happened (Figure 5h, j).

Figure 5. Photographs of thin sections of rock samples examined under optical microscope **(a)** KY9, Serpentinite, XPL **(b)** KY10, Serpentinite, PPL **(c)** KY6, Basalt, XPL **(d)** KY7, Basalt, XPL **(e)** KY13, Dacite, XPL **(f)** KY12, Dacite, PPL **(g)** KY8, Troctolite, XPL **(h)** KY3, Sandstone, XPL **(j)** KY4, Sandstone, XPL.

3.2. XRD Analyses

Quartz, feldspar, calcite, gypsum and halite are found in whole rocks of eleven samples taken from the Tuzluca Formation; Chlorite, smectite and palygorskite minerals were detected in the clay fractions (Table 1). In the samples, gypsum is 40-50%, halite 5-10%, quartz and calcite 20-30%, smectite and palygorskite 10-20%. 10% are other minerals. X-ray diffractograms of representative samples were put in Figure 6.

XRD analyses were performed on 3 rock samples of Turabi Formation and 18 rock samples of Çincavat Formation taken along the measured stratigraphic section of Turabi village. Quartz, feldspar, calcite, gypsum in whole rock; chlorite, smectite and illite/mica minerals in clay fractions were detected. Unlike the Tuzluca (salt pit) samples, palygorskite is not found in these formations. The mineral contents of the Çincavat Formation rocks are 40-50% quartz, 20-30% gypsum, 30-40% smectite and 10% other minerals. In the Turabi Formation, roughly 40-50% quartz, 10-20% feldspar, 10-20% calcite, 10-20% smectite and 10% other minerals (Table 1).

Table 1. Mineralogical composition of samples. Qz: Quartz, Fsp: Feldspar, Cal: Calcite, Gp: Gypsum, HI: Halite, Plg: Palygorskite, Chl: Chlorite, Sme: Smectite, Ilt/Mca: Illite and mica, acc: Accessory, +: Mineral abundance ratio, +: 10-30%; acc: ±10% (Mineral name abbreviations were taken from [22]).

Formation	Sample No	Lithology	Qz	Fsp	Cal	Gp	HI	Plg	Chl	Sme	Ilt/Mca
Tuzluca	TTM-1	Gypsum	acc	acc	acc	++++	++	acc	acc		
Tuzluca	TTM-3	Gypsum	acc	acc	acc	+++++					
Tuzluca	TTM-4	Claystone	+++	acc	acc			+	acc	+	
Tuzluca	TTM-5	Marl	++	acc	++			+	acc	+	
Tuzluca	TTM-6	Claystone	++	acc	++			+	acc	+	
Tuzluca	TTM-7	Gypsum	acc	acc	acc	+++++					
Tuzluca	TTM-8	Gypsum	acc	acc	acc	+++++					
Tuzluca	TTM-10	Claystone	acc	acc	acc	+++	++	acc	acc		
Tuzluca	TTM-11	Claystone	++	acc	++			+	acc	+	
Tuzluca	TTM-12	Claystone	++	acc	++			+	acc	+	
Tuzluca	TTM-14	Gypsum	acc	acc	acc	+++++					
Çincavat	TÇ-2	Mudstone	++	acc	++				acc	+	
Çincavat	TÇ-3	Mudstone	+++	acc	acc				acc	+ +	
Çincavat	TÇ-4	Mudstone	++	acc	++				acc	+	
Çincavat	TÇ-5	Mudstone	+++	acc	+				acc	+	
Çincavat	TÇ-6	Mudstone	+	++	acc				acc	++	
Çincavat	TÇ-7	Mudstone	++	+	acc				acc	++	
Çincavat	TÇ-9	Mudstone	++	+	acc				acc	++	
Çincavat	TÇ-10	Gypsum	+	acc	acc	+++			acc	+	
Çincavat	TÇ-11B	Gypsum	acc	acc	acc	+++++					
Çincavat	TÇ-13	Mudstone	+++	acc	acc				acc	++	
Çincavat	TÇ-14	Mudstone	+++	acc	acc				acc	+	
Çincavat	TÇ-15	Mudstone	+	acc	acc	+			acc	+++	
Çincavat	TÇ-16	Mudstone	++	acc	acc	+			acc	++	
Çincavat	TÇ-17	Mudstone	+	acc	acc	++			acc	++	
Çincavat	TÇ-18	Siltstone	+++	acc	acc	++					
Çincavat	TÇ-19	Siltstone	++	acc	acc	++			acc	+	
Çincavat	TÇ-20	Siltstone	++	acc	acc	+			acc	++	
Çincavat	TÇ-21	Siltstone	++	acc	acc	++			acc	+	
Turabi	TÇ-31	Claystone	++	acc	acc	++				++	
Turabi	TÇ-33	Sandstone	+++	++						acc	
Turabi	TÇ-35	Marl	++	acc	++	+			acc	acc	acc

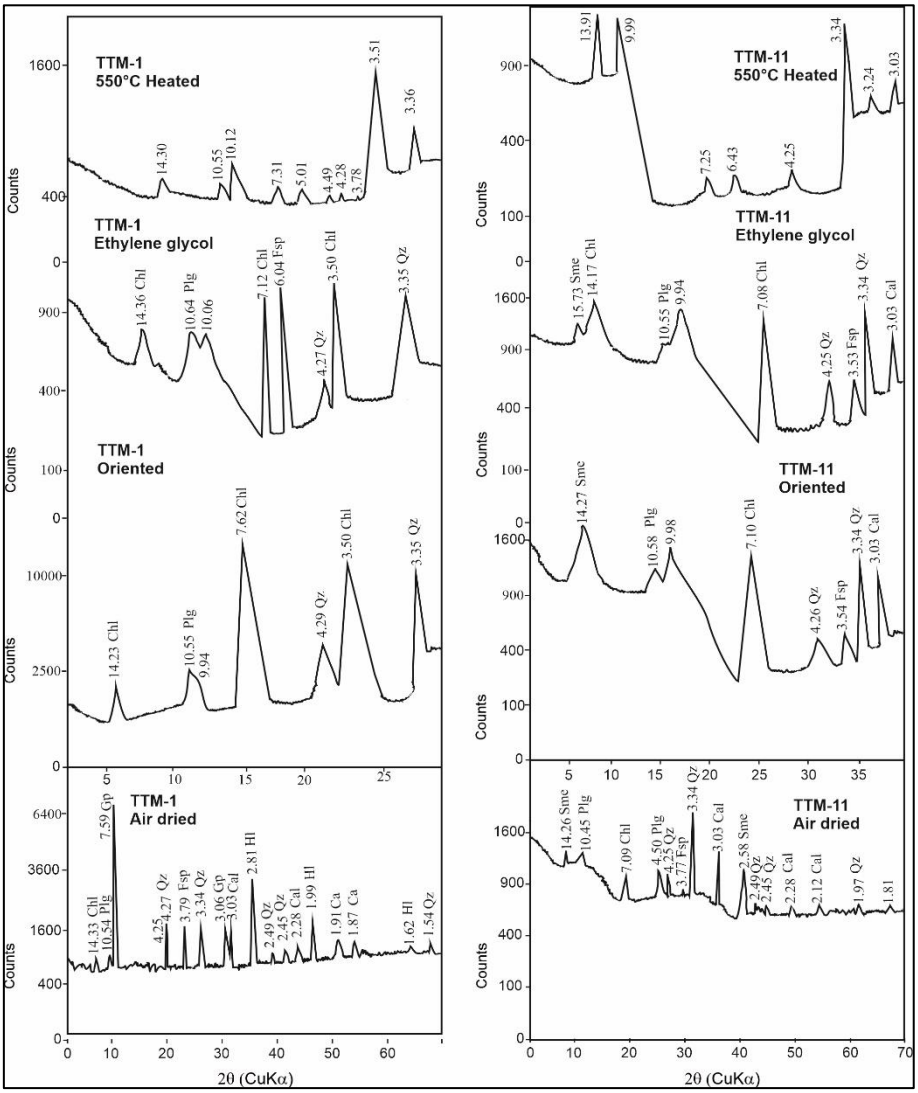

Figure 6. XRD diffractograms of TTM-1 and TTM-11 samples of the Tuzluca Formation (see explanations of Table 1 for abbreviations)

3.3. SEM-EDS Study

Scanning electron microscopy (SEM) and microchemical analysis (EDS) studies were performed on four samples. Among these samples, TTM-1 (Tuzluca) is gypsum, TTM-6 (Tuzluca) and TTM-11 (Tuzluca) are claystone, and TÇ-3 (Çincavat) is mudstone. SEM microphotographs of these samples with numbers and lithologies of them are given in Figure 7.

Gypsum mineral has a prismatic-looking structure. EDS analysis shows Ca (31,49%) and S (21,06%) (Figures 7a, b).

The feldspar grain appears to be surrounded by blocky, well-developed, planar outgrowths. EDS analyses show Si (34,93%) and Al (11,69%) values. In SEM analysis, prismatic-shaped gypsum minerals surrounded the smooth-edged feldspars (Figure 7b).

Chlorite mineral (EDS analysis Si (24.21%), Al (8.96%), Mg (3.07%), Fe (30.54%)), which is an accessory mineral, has developed around the cubic halite mineral (EDS analysis Na (13.28%), Cl (10.47%)) (Figure 7c).

There are calcite minerals (EDS analysis Ca (58.90%), O (30.47%)) around the smooth-edged quartz grain (EDS analysis Si (38.79%), O (52.76%)) (Figure 7d).

The smectite mineral, which consists of leafy plates and has a honeycomb appearance, is seen together with the fibrous palygorskite mineral (Figure 7e, f). While the EDS analysis results of the smectite are Si (24.48%), Al (8.79%), Mg (5.01%), Fe (27.90%), those of the palygorskite are Si (24.72%), Al (9.62%), Mg (6.17%), Fe (7.75%)).

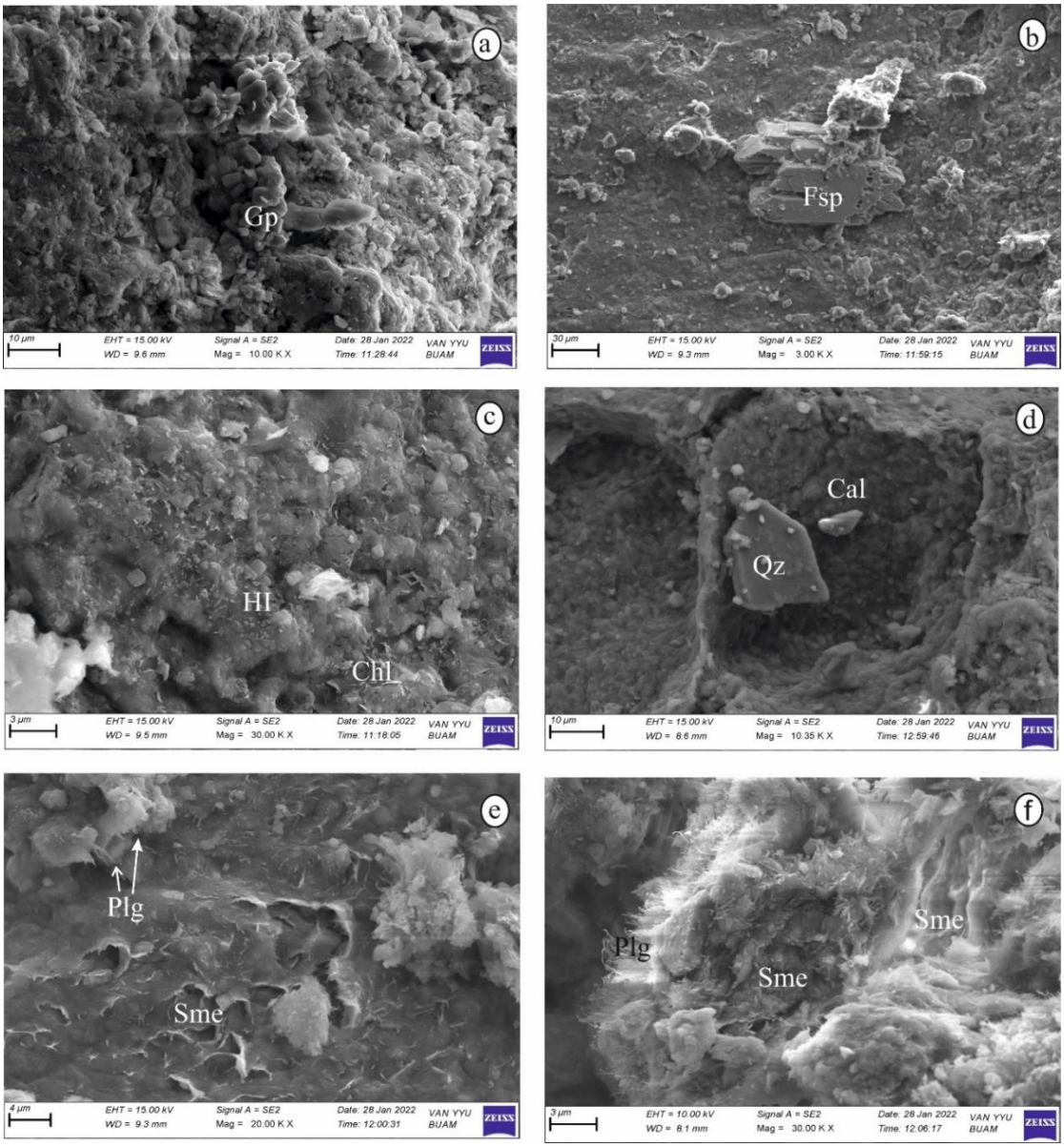

Figure 7. SEM microphotographs of samples **(a)** TTM-1, gypsum **(b)** TTM-1, gypsum **(c)** TTM-1, claystone **(d)** TÇ-3, mudstone **(e)** TTM-6, claystone **(f)** TTM-11, claystone

3.4. Geochemistry

Major oxide and trace elements results of samples of the study area are put in Table 2.

Table 2. Major oxides (% weight) and trace elements (ppm) contents of the samples (Gp: Gypsum, Clst: Claystone, Mdst: Mudstone, Sltst: Siltstone, Ss: Sandstone)

	Tuzluca Formation					**Çincavat Formation**				**Turabi Formation**			
Major oxide (% weight)	**TTM-3 (Gp)**	**TTM- 10 (Clst)**	**TTM-12 (Clst)**	**TTM-14 (Gp)**	**Avg.**	**TÇ-6 (Mdst)**	**TÇ-14 (Mdst)**	**TÇ-18 (Sltst)**	**Avg.**	**TÇ-31 (Clst)**	**TÇ-33 (Sst)**	**TÇ-35 (Marl)**	**Avg.**
SiO_2	25.73	25.42	46.85	30.14	32.0	52.44	55.84	54.76	54.34	54.62	59.65	50.36	54.88
Al_2O_3	5.83	4.39	11.82	7.53	7.39	14.4	13.35	13.47	13.74	15.61	10.9	8.99	11.83
Fe_2O_3	3.62	3.28	6.86	3.43	4.30	8.54	7.26	8.21	8.00	7.07	5.47	4.73	5.76
MgO	3.69	10.15	7.28	4.02	6.28	3.75	2.93	2.55	3.07	2.13	2.22	1.39	1.92
CaO	26.2	27.23	7.72	14.12	18.31	2.42	1.92	2.30	2,21	1.18	1.33	13.8	5.43
Na_2O	0.07	0.05	0.73	0.10	0.20	0.80	1.59	1.01	1.14	0.94	3.27	2.33	2.18
K_2O	1.53	1.23	2.72	1.94	1.85	1.61	1.79	1.71	1.70	1.40	2.31	2.88	2.20
TiO_2	0.35	0.23	0.54	0.42	0.39	0.64	0.73	0.71	0.69	0.63	0.41	0.43	0.49
P_2O_5	0.13	0.09	0.13	0.11	0.12	0.10	0.12	0.11	0.11	0.09	0.14	0.09	0.11
SO_3	15.75	4.54	5.36	19.09	11.18	0.70	0.20	2.03	0.98	2.66	2.38	1.14	2.06
Cr_2O_3	0.01	0.06	0.02	0.01	0.01	0.01	0.02	0.09	0.01	0.01	0.03	0.01	0.01
V_2O_5	0.01	0.01	0.02	0.01	0.01	0.02	0.03	0.02	0.02	0.02	0.01	0.01	0.01
CI	0.26	0.17	0.59	0.17	0.30	0.45	0.62	0.015	0.36	0.27	1.13	0.01	0.47
MnO	0.07	0.14	0.07	0.03	0.081	0.09	0.16	0.10	0.12	0.01	0.04	0.10	0.05
Al_2O_3/TiO_2	16.6	19.00	21.8	17.9	18.9	22.5	18.2	18.9	19.9	24.7	26.5	20.9	24.0
LOI	14.82	21.83	9.83	16.3	15.69	13.82	13.83	12.93	13.52	13.82	10.83	13.93	12.86
Total	99.36	99.24	99.34	99.32	99.32	99.22	99.24	99.76	99.40	99.24	99.26	99.32	99.27
Trace elements (ppm)													
Co	14.0	27.8	42.4	39.9	31.02	39.6	50.3	32.3	40.43	41.9	49.7	30.5	40.7
Ni	106.2	71.3	235	160.1	143.15	86.2	75.3	83.8	81.76	20.7	79.4	25.7	41.9
Cu	24.0	19.0	24.2	49.4	29.15	71.3	29.4	69.2	56.63	35.8	45.9	17.2	32.9
Zn	33.0	27.6	59.9	37.2	39.42	78.3	76.6	91.7	82.2	51.5	64.5	32	49.3
Ga	7.0	6.8	12.3	9.8	8.97	17.7	15.8	18.8	17.43	19.3	13.4	12.1	14,9
Ge	0.4	0.8	0.7	0.4	0.57	1.8	1.1	1.5	1.46	0.9	1.6	0.5	1.0
As	9.8	20.2	5.6	5.0	10.15	5.6	4.5	5.2	5.1	2.7	9.9	4.8	5.8
Se	0.8	0.3	0.3	0.5	0.47	0.5	0.2	0.3	0.33	0.6	1.4	0.3	1.2
Br	4.6	12.6	7.1	4.3	7.15	20.5	12.8	1.8	11.7	6.7	26.2	1.1	11.3
Rb	29.9	25.2	52.2	32.6	34.9	62.7	53.9	67.5	61.3	67.2	57.3	51.9	58.8
Sr	5051	316	1021	213	1650	235	213	233	227	145	308	233	228
Hf	3.6	2.7	3.0	3.4	3.17	3.8	2.9	3.7	3.46	4.1	3.1	2.4	3.2
Zr	95	52.4	113.6	47.6	77.3	138.7	174.1	147.2	153.0	143.2	104.9	102.8	116.9
Nb	6.6	5.7	11.1	6.7	7.52	14.1	17.7	14.3	15.36	11.7	5.5	11.0	9.4
Mo	3.7	4.5	3.4	4.1	3.92	4.3	7.6	3.5	5.13	2.1	3.1	3.5	2.9
Cd	0.8	0.9	0.8	0.8	0.82	0.8	1.1	0.8	0.9	0.8	0.7	0.6	0.7
In	0.9	0.8	0.9	0.8	0.85	0,9	0.9	0.8	0.86	0.8	0.7	0.9	0.8
Te	1.2	1.2	1.3	1.2	1.22	1.2	1.2	1.2	1.2	1.1	1.2	1.3	1.2
I	1.9	1.7	2.1	3.6	2.32	2.2	2.1	2.2	2.16	2.1	2.3	3.5	2.63
Cs	3.5	3.5	3.6	6.7	4.32	3.7	3.6	3.7	3.66	3.6	3.7	3.7	3.66
Ba	358	76.5	465.9	91.3	248.7	522.1	298.1	538	452.7	410.6	874.2	488.1	590.3
La	7.2	7.5	13.8	15.8	11,07	21.4	24.5	24.3	23.4	7.4	13.8	13.6	11.6
Ce	10.0	26.4	28.0	20.0	21.1	52.2	31.3	52.4	45.3	26.6	26.4	23.5	25.5
Y	0.7	7.8	10.8	6.1	6.35	19.6	20.1	24	21.23	8.6	15.2	13.1	12.3
Ta	4.4	3.0	3.8	4.3	3.87	4.5	3.2	4.6	4.1	3.3	3.7	3.2	3.4
W	3.6	2.4	3.5	3.0	3.12	2.7	6.4	2.7	3.93	2.2	40.7	40.3	27.7
Hg	1.0	0.7	0.8	0.7	0.8	0.7	0.7	0.7	0.7	0.7	0.9	0.8	0.8
Tl	1.0	0.8	0.8	0.7	0.82	0.8	0.6	0.8	0.73	0.7	1.3	0.8	0.93
Pb	12.6	8.2	3.4	4.3	7.12	11.3	10.1	14.3	11.9	9.6	9.7	9.5	9.6
Bi	0.7	0.6	0.6	0.6	0.62	0.5	0.5	0.5	0.5	0.5	0.5	0.5	0.5
Th	2.8	2.5	2.1	2.2	2.4	9.9	6.5	8.5	8.3	8.7	5.3	5.4	6.46
U	13.3	14.1	17.7	8.4	13.7	8.8	16.9	8.9	11.12	7.2	6.8	7.7	7.23
Sr/Ba	14.08	4.13	2.19	2.33	6.65	0.45	0.71	0.43	0.50	0.35	0.35	0.47	0.38

In samples with high SiO_2 content, quartz accompanies clay minerals.

The increase in Fe/Al oxide ratios is noteworthy in the rock analysis of the Çincavat Formation. These increases indicate the input of terrestrial sediments, and the resedimentation under high energy conditions during maximum flooding [24].

The lower amounts of Na 1.09% and the more common Mg 4.01% in all samples prove that an ancient playa lake developed. Mg-salts or Mg-Al silicates such as palygorskite have been reported from various paleo-lakes [25].

SiO_2 has positive correlations with Al_2O_3 (R^2=0.74), Fe_2O_3 (R^2=0.63), Na_2O (R^2=0.56), TiO_2 (R^2=0.53), while has a negative correlation with MgO (R^2=0.36) (Figure 8).

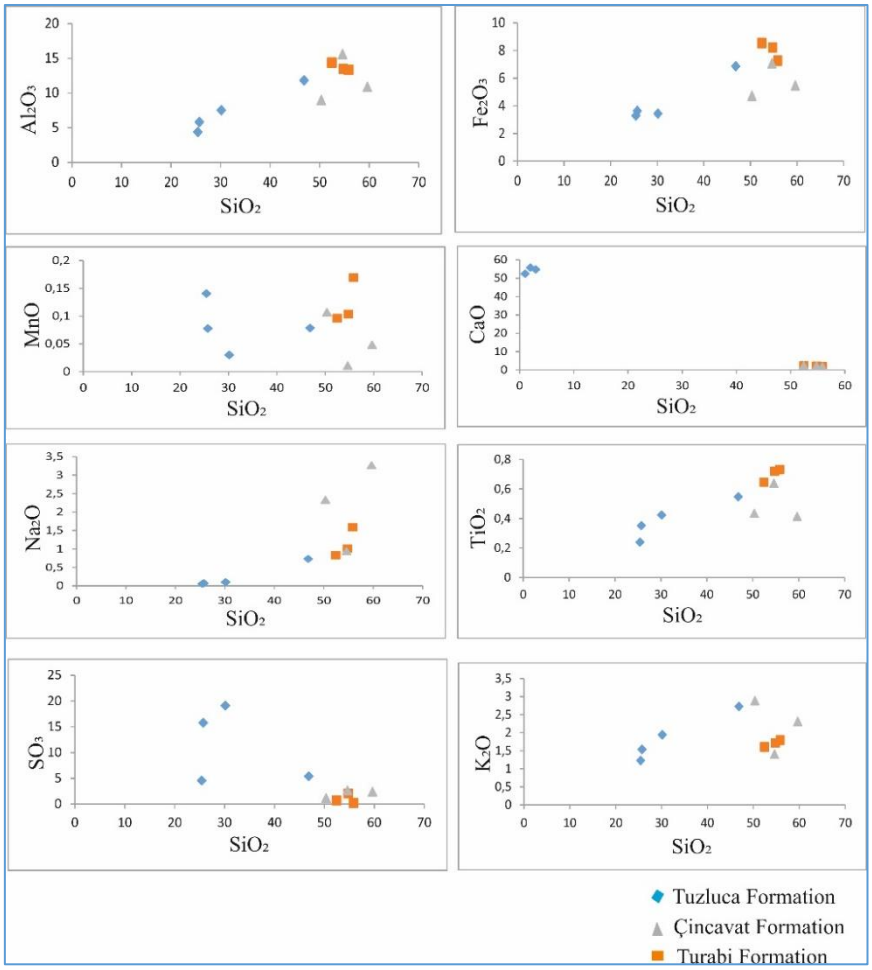

Figure 8. Correlation plots of SiO_2 versus Al_2O_3, Fe_2O_3, MnO, CaO, Na_2O, TiO_2, SO_3 and K_2O

In the chemically analyzed samples, trace elements Sr (avg. 227.4-1650.3 ppm), Ba (avg. 248.0-590.9 ppm), Rb (34.9-61.3 ppm), Co (31.02 ppm). 40,7 ppm), Ni (41.9-143.1 ppm), Cu (34.9-58.8 ppm), Zr (77.3-153.3 ppm), Zn (39,2-82,2 ppm) percentage rates were determined to be high (Table 2). The reason why these values are high is due to the influence of factors (hydrothermal solutions, ground-surface water and confined-closed reducing environment conditions, etc.) affecting the mineralogical and geochemical character of the lake water in different regions (lake shore, lake plain and deep lake area, etc.) during the evaporation of the region [27, 28, 30; 23].

Correlation plots of Al_2O_3 vs. Rb, Th, Zr and Fe_2O_3 vs. Zn values were drawn for the samples where elemental determination was made (Figure 9). The high positive correlation between Al_2O_3 and Rb, Th, Zr indicates that there were siliciclastic inputs into the depositional environment [30-33; 12]). The high positive correlation between Al_2O_3 and Rb (R^2=0.88), Th (R^2=0.65), Zr (R^2=0.73) in the analyzed samples and the feldspar and quartz minerals detected in XRD and SEM images support this view. The presence of a high positive correlation (R^2=0.80) between Zn and Fe_2O_3 indicates that the Zn element is of biological origin. In addition, Zn, Cu, Ni and Co elements and their high concentrations indicate the presence of microorganisms in the environment and the high activity of these organisms [12].

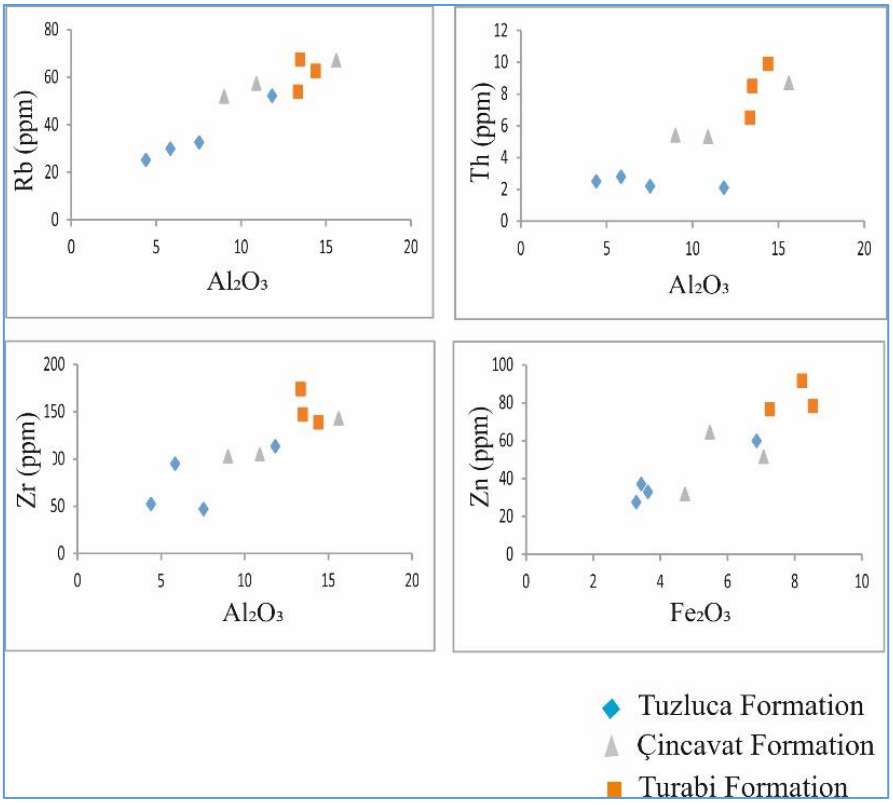

Figure 9. Correlation plots between specific trace elements and major oxides

4. DISCUSSION

In previous studies, it was interpreted that the rocks that constitute the subject of this study were formed in continental environments. While evaporites formed in marine environments have a Sr content of 1000-3000 ppm [34], evaporites in terrestrial environments have a Sr content of 50-200 ppm [35]. In the elemental analyses, Sr content shows values between (an average of 228.8-5051 ppm) (Table 2). Abdioğlu et al. [34] point out that simultaneous volcanism around the basin can increase Sr input into the environment and cause much higher Sr content than normal seawater. In addition, Sr content is also affected by hydrothermal solutions. The fact that there was no simultaneous volcanism during the period when the rocks were formed was interpreted as the excess in Sr content due to the effect of hydrothermal solutions.

Because low MgO values indicate detrital origin [36] the XRF results of samples of Turabi and Çincavat Formations show that the clay minerals (except smectite) are of detrital origin.

Carbonate precipitation is common in areas subject to frequent evaporation and solution concentration [37-39]. Calcite and dolomite are often the first minerals to precipitate during the concentration process. Dolomite has not been identified in the basin rocks. Calcite usually contains less than 5% mol $MgCO_3$. This is because it precipitates from more dilute solutions with low Mg/Ca ratios [40]. In the Tuzluca Formation, the Mg/Ca ratio is the lowest and the calcite ratio is higher.

Clay mineral assemblages are primarily a function of climate, and these minerals are affected by weathering time, slope, water-rock ratio, and water chemistry [41-45]. The fact that smectite is the dominant clay mineral in all three formations is related to an advanced degree of hydrolysis and shows that the climate is generally hot and humid [41-43]. However, the observation of illite and chlorite along with smectite in the Turabi Formation indicates that the environment was occasionally under cold and/or dry conditions [46]. In the Çincavat Formation, the dominance of smectite and the presence of trace amounts of chlorite indicate that the climate is warmer and more humid. It is interesting that palygorskite and magnesium smectite were identified along with gypsum in the Tuzluca Formation samples. The formation of fibrous clay forms such as palygorskite along with Mg-smectite in saline lake environments requires a hot climate, severe hydrolysis and evaporation. While high salinity primarily causes the formation of various salts, high alkalinity in the volcanic environment mostly causes the formation of zeolites [41]. The fact that volcanic material and zeolite minerals were not determined in this study was interpreted as the absence of volcanism in the basin during the period when the studied formations were formed.

The Sr/Ba ratio is an important indicator of paleosalinity [47, 48]. The classification is as follows: Sr/Ba <0,5 indicates brackish water, 0,5 <Sr/Ba <1 indicates a brackish lake, and Sr/Ba >1 indicates a saline water environment [49]. Tuzluca Formation Sr/Ba ratio (mean:6,65) indicates a saline water environment, Çincavat Formation Sr/Ba ratio (mean: 0,5) indicates a brackish lake environment and a brackish water environment, Turabi Formation Sr/Ba ratio (mean:0,38) indicates a brackish water environment.

5. CONCLUSIONS

In this study, the Miocene lithostratigraphic units (Turabi, Çincavat and Tuzluca formations) outcrop in the Tuzluca section of Neogene Kağızman-Tuzluca Basin were studied. The units are represented by evaporitic, carbonate and clayey rocks. Evaporites are common in Tuzluca Formation. Quartz, feldspar, mica, calcite, gypsum and halite minerals were determined in whole rock compositions of the samples. Smectite, illite, chlorite and paligorskite minerals were found in the clay fractions. Because of low MgO values and the increase in Fe/Al oxide ratios of the Çincavat Formation, clay minerals (except smectite) are interpreted as detrital origin. Palygorskite was only detected in the clay fractions of the samples of the Tuzluca Formation. Gypsum, halite, calcite and palygorskite are interpreted as authigenic while chlorite, illite, quartz, feldspar and mica were detrital. These minerals were formed in terrestrial environments without volcanic contribution. The high positive correlation between Al_2O_3 and Rb, Th, Zr indicates that there were siliciclastic inputs into the depositional environment. Clay minerals (smectite, chlorite, illite, palygorskite) suggest that the environmental conditions were alkaline. Smectite is the dominant clay mineral in the rock samples and indicate that the conditions were generally hot and humid. It also shows that there was severe hydrolysis throughout the basin. In addition, the presence of illite in the Turabi Formation signifies that cold and/or dry conditions developed in the basin sometimes. Palygorskite which is only detected in rock samples of Tuzluca Formation implies that the climate conditions were semi-arid from time to time during the period when this formation was formed. Sr/Ba ratios suggest a saline water environment for the Tuzluca formation, both a brackish lake environment and a brackish water environment for Çincavat Formation and a brackish water environment for Turabi Formation. The presence of a high positive correlation (R^2=0.80) between Zn and Fe_2O_3 signifies that

the Zn element is of biological origin. In addition, Zn, Cu, Ni and Co elements and their high concentrations suggest the presence of microorganisms in the environment and the high activity of these organisms.

ACKNOWLEDGEMENTS

This paper was prepared by using the second author's master's thesis [50]. The thesis has been supported by Van Yüzüncü Yıl University Scientific Research Projects Coordination Unit under grant number FYL-2021-9448.
The authors thank the reviewers for their constructive input to the improvement of this article.

CONFLICT OF INTEREST

The authors stated that there are no conflicts of interest regarding the publication of this article.

AUTHORSHIP CONTRIBUTIONS

Türker YAKUPOĞLU and Enver KARASU contributed to the study conception and design equally. All authors read and approved the final manuscript.

REFERENCES

[1] Şengör AMC. Cross faults and differential stretching of hanging walls in regions of low angle normal faulting: examples from western Turkey. Geolsoc 1987; 28:575–589.

[2] Purvis M, Robertson AHF. Sedimentation of the Neogene–Recent Alaşehir (Gediz) Continental Graben System used to Test Alternative Tectonic Models for Western (Aegean) Turkey. Sed Geol 2005; 173:373–408.

[3] Purvis M, Robertson AHF. Miocene sedimentary evolution of the NE–SW-trending Selendi and Gördes Basins, W Turkey: Implications for Extensional Process. Sed Geol 2005; 174:31–62.

[4] Çiftçi NB, Bozkurt E. Structural evolution of the Gediz Graben, SW Turkey: Temporal and Spatial Variation of the Graben Basin. Basin Res 2010; 22:846–873.

[5] Ayyıldız T, Varol B, Karakaş Z, Sözeri K. Basic Geochemical Characteristics of Lacustrine Rocks in the Neogene Kağızman–Tuzluca Basin, Northeastern Turkey, J. Pet. Expl. Pro. Tec. 2019: 9; 141-157.

[6] Yılmaz O, Şener M. Investigation of well samples taken from Erzurum-Pasinler, Erzincan-Çayırlı, Kars-Tuzluca and Malatya-Haeılar by X-ray diffraction. Türk Jeo Kurul Bült 1984; 27:31–40.

[7] Yılmaz O. Geology, mineralogy and petrography of the Kağızman (Kars – Tuzluca (Iğdır) tuz yataklarının Kağızman (Kars)–Tuzluca (Iğdır) salt beds. MSc. Dokuz Eylül University, İzmir, Türkiye, 2007.

[8] Karakaş Z, Varol B, Ayyıldız T, Sözeri K. Occurrence of Clay Minerals Associated with Caliche in the Neogene Çincavat Formation (Tuzluca Basin, NW of Iğdır). In: Euroclay 2011 European Clay Conference; 26 June- 01 July 2011: Antalya, Türkiye. 252.

[9] Güngör-Yeşilova P, Yeşilova Ç. Depositional Basin, Diagenetic Conditions and Source of Miocene Evaporites in the Tuzluca Basin in Northeastern Anatolia, Turkey: Geochemical Evidence. Geo. Int. 2021; 59: 1293–1310.

[10] Şaroğlu F, Yılmaz Y. Geological Evolution and Basin Models During the Neotectonic Episode in Eastern Anatolia. Bul Min Res Expl Inst. 1986; 107: 61–83.

[11] Varol B, Ayyıldız T, Karakaş Z, Sözeri K. Fault-İnduced "Pull-Apart" Terrestrial Depositional Model in the Igdir-Kagizman Neogene Basin, Eastern Turkey. 27th IAS Meeting Sediment; 20-23 September 2009; Alghero, Italy. pp 35–39.

[12] Ayyıldız T, Varol B, Karakaş Z, Sözeri K. Miocene Evaporites in the Intermountain Tuzluca-Iğdır Neogene Basin, Eastern Turkey. EGU General Assembly; 22-27 April 2012; Vienna, Austria.

[13] Varol B, Şen Ş, Ayyıldız T, Sözeri K, Karakaş Z, Métais G. Sedimentology and Stratigraphy of Cenozoic Deposits in the Kağizman-Tuzluca Basin, Northeastern Turkey. Inter. Jour. of Scien. 2016; 105:107–137.

[14] Koçyiğit A, Yılmaz A, Adamia S, Kuloshvili S. Neotectonics of East Anatolian Plateau (Turkey) and Lesser Caucasus: implication for transition from thrusting to strike-slip faulting. Geo. Acta 2001; 14:177–195.

[15] Şen Ş, Antoine PO, Varol B, Ayyıldız T, Sözeri K. Giant rhinoceros Paraceratherium and other vertebrates from Oligocene and middle Miocene deposits of the Kağizman–Tuzluca Basin, Eastern Turkey. Naturwissenschaften 2011; 98: 407–423.

[16] Sancay RH. Palynostratigraphic and palynofacies investigation of the Oligocene-Miocene units in the Kars-Erzurum-Muş Subbasins (Eastern Anatolia). MSc, Middle East Technical University, Ankara, Turkey, 2012.

[17] Hanawalt JD, Rinn HW, Frevel LK. Chemical Analysis by X-Ray Diffraction. Anl Chem 1938; 10:475-512.

[18] Brindley GW, Brown G. Crystal Structures of Clay Minerals and their X-ray Identification. London, LD, England: Min Soc, 1980.

[19] Wilson MJ. A Handbook of Determinative Methods in Clay Mineralogy. London, LD, England: Blackie, 1987.

[20] Moore DM, Reynolds RC. X-ray Diffraction and the Identification and Analysis of Clay Minerals. 2nd ed. Illinois, USA: Oxford Su Press, 1997.

[21] Welton, JE. SEM Petrology Atlas. Tulsa, Oklahama, USA: AAPG Press, 1984.

[22] Whitney LD, Evans WB. Abbreviations for names of rock-forming minerals. USA Min 2010; 95: 185-187.

[23] Güngör-Yeşilova P, Tekin E. Geochemical and Geostatistical Investigation of Upper Miocene Evaporites in the Polatlı-Sivrihisar Neogene Basin (Demirci Village, NE Sivrihisar; Central Anatolia, Turkey). Tür Jeo Bül 2007; 50: 71-94.

[24] Perkins BR, Piper DZ. Life cycle of the Phosphoria Formation: from Deposition to the Post-Mining Environment. Amsterdam, Holland: Elsevier Sci, 2004.

[25] Smykatz-Kloss W, Roy PD. Evaporite Mineralogy and Major Element Geochemistry as Tools for Palaeoclimatic Investigations in Arid Regions: A Synthesis. UNAM 2010; 62: 379-390.

[26] Crook KAW. Lithogenesis and Geotectonics: the Significance of Compositional Variations in Flysch Arenites (graywackes), in Dott, R.H., Shaver, R.H. (eds.), Modern and Ancient Geosynclinal Sedimentation. SEPM 1974; 19: 304–310.

[27] Emelyanov EM, Shimhus KM. Geochemistry and Sedimentology of the Mediterranean Sea. Paris, France: Springer, 1986.

[28] Tekin E, Varol B. Petrographic investigation of celestine deposits in the Sivas Basin (Central Anatolia). A. Suat Erk Jeo. Sempozyumu 1993; 319-327.

[29] Tekin E, Ayan Z, Varol B. Fluid inclusion studies and microtextural characteristics of Sivas-Ulaş celestite deposits (Tertiary) Türk Jeol Bült 1994; 37: 61-76.

[30] Pye K, Krinsley DH. Diagenetic Carbonate and Evaporite Minerals in Rotliegend Aeolian Sandstones of the Southern North Sea: Their Nature and Relationship to Secondary Porosity. Clay Min 1986; 21:443–457.

[31] Haug GH, Gunther D, Peterson LC, Sigman DM, Highen KA, Aeschlimann B. Climate and the Collapse of Maya Civilization. AAAS 2003; 299: 1731–1735.

[32] Guo P, Chiyang L, Peng W, Ke W, Haili Y, Bei Li. Geochemical behavior of rare elements in Paleogene Saline Lake Sediments of the Qaidam Basin, NE Tibetan Plateau. Carb Evap 2019; 34: 359-372.

[33] Reinhardt N, Proenza JA, Villanova-de-Benavent C, Aiglsperger T, Bover-Arnal T, Torro L, Salas R, Dziggel A. Geochemistry and Mineralogy of Rare Earth Elements (ree) in Bauxitic Ores of the Catalan Coastal Range, NE Spain, MDPI 2018; 8:562.

[34] Abdioğlu E, Arslan M, Helvacı C, Gündoğan İ, Temizel İ, Aydınçakır D. Geochemistry of Miocene evaporites from the Aşkale (Erzurum, Eastern Turkey) area: Constraints for Paleo-Environment. Bull Miner Res and Explor 2021; 165: 1-45.

[35] Krauskopf KB, Bird DK. Introduction to Geochemistry. New York, NY, USA: McGraw-Hill, 1994.

[36] Fisher RS. Clay Minerals in Evaporite Host Rock, Palo Duro Basin, Texas Panhandle. SEPM 1988; 58: 836-844.

[37] Fehrenbacher JB, Wilding LP, Odell RT, Melsted SW. Characteristics of solonetzic soils in Illinois. SSSA 1963; 27: 421– 431.

[38] Mahjoory RA. The Nature and Genesis of Some Salt-Affected Soils in Iran Soil. SSSA 1979; 43: 1019–1024.

[39] Kohut CK, Dudas M.J. Evaporite Mineralogy and Trace-Element Content of Salt Affected Soil in Alberta. Can. J. Soil. Sci. 1995; 73 :399–409.

[40] Furquim SAC, Graham RC, Barbiero C, Queiroz Neto, JP, Vidal-Torrado P. Soil Mineral Genesis and Distribution in a Saline Lake Landscape of the Pantanal Wetland, Brazil. Geoderma 2010; 154: 518–528.

[41] Chamley H. Clay Sedimentology. Verlag, Berlin, German: Springer, 1989.

[42] Nesbitt HW, Young GM. Formation and Diagenesis of Weathering Profiles. Jour Geol 1989; 97: 129–147.

[43] Nesbitt, HW, Fedo CM., Young G.M. Quartz and Feldspar Stability, Steady and Nonsteady-State Weathering, and Petrogenesis of Siliciclastic Sands and Muds. Jour Geol 1997; 105: 173–191.

[44] Fürsich FT, Singh IB, Joachimski M, Krumm S, Schlirf M, Schlirf S. Palaeoclimate Reconstructions of the Middle Jurassic of Kachchh (western India): an İntegrated Approach Based on Palaeoecological, Oxygen Isotopic, and Clay Mineralogical Data. Palaeo 2005; 217: 289–309.

[45] Kovacs J, Raucsık B, Varga A, Ujvarı G, Varga G, Ottner F. Clay mineralogy of red clay deposits from the central Carpathian Basin (Hungary): implications for Plio-Pleistocene chemical weathering and palaeoclimate. TÜBİTAK 2013; 22: 414-426.

[46] Chamley H, Masse JP. Sur la Signification Des Min´eraux Argileux Dans Les S´ediments Barremiens et B´edouliens de Provence. In 9th Sedimentology Cong; 1975; 1:25-29

[47] Yang R, Fan A, Van-Loon AJ, Han Z, Zavala C. The Influence of Hyperpycnal flows on the Salinity of Deep-Marine Environments, and Implications for the Interpretation of Marine Facies. Mar. Petrol. Geol. 2018; 98:1-11

[48] Yun J, Guoqiang S, Shile P, Yetong W, Shuncong Z. Sedimentary Environment Analysis of Eocene in Pingtai Area of Qaidam Basin, China. Res. Squ. 2021.

[49] Dera G, Pellenard P, Neige P, Deconinck JF, Pucéat E, Dommergues JL. Discussion of Sedimentary Environment and Its Geological Enlightenment of Shanxi Formation in Ordos Basin. Act. Petrol. Sin. 2011; 27:2213–2229.

[50] Karasu E. Determination of mineralogical and geochemical characteristics of Miocene aged rocks outcropped around Tuzluca (Iğdır/Türkiye). MSc, Van Yüzüncü Yıl University, Van, Türkiye, 2022.